A new mechanism for the Favorskii rearrangement†

Noriko Tsuchida, Shoko Yamazaki and Shinichi Yamabe*

Received 21st April 2008, Accepted 30th May 2008
First published as an Advance Article on the web 30th June 2008
DOI: 10.1039/b806577b

The title reaction was investigated by the use of ONIOM-RB3LYP calculations. A reaction system composed of α-chlorocyclohexanone, a methoxide ion and 8 MeOH solvent molecules was adopted. Two reaction channels, the semibenzilic acid mechanism (A) and cyclopropanone mechanism (B), were compared. B is found to be more favorable than A. The rate-determining step of B is the $(MeOH)_3$ addition transition state (TS3B) to the cyclopropanone intermediate. While TS3B involves a concerted function of MeO^- addition and proton relays, it has a large activation energy. A new route was found, where the chloride ion evolved at the cyclopropane formation step (TS2B) works as a nucleophile to the cyclopropanone intermediate. Thus, a cyclopentane-carbonyl chloride intermediate is formed with a small activation energy. A new cyclopropanone mechanism is proposed.

1 Introduction

The base-catalyzed conversion of α-haloketones to carboxylic acid derivatives is known as the Favorskii reaction.[1–3] It is widely used for the synthesis of highly branched carboxylic acid[4] and cage compounds.[5] The reaction has been subjected to extensive mechanistic studies.[6–8] There is strong evidence that the rearrangement involves the open 1,3-dipolar form of cyclopropanone and/or the cyclopropanone as a reaction intermediate (Scheme 1).[6] There is also a related mechanism that can operate in the absence of an acidic α-hydrogen; it is known as the "semibenzilic" rearrangement (Scheme 2).

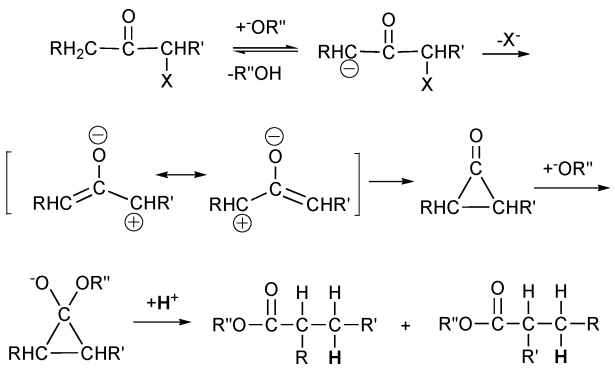

Scheme 1 A Favorskii rearrangement of an aliphatic ketone. $R''O^-$ is an alkoxide, and X^- is a halide ion. The cyclopropane intermediate is involved.

The net structural change is the same for both mechanisms. The energy requirements of the cyclopropanone and semibenzilic mechanisms may be fairly closely balanced. Examples of the

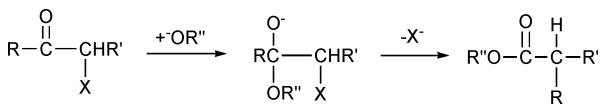

Scheme 2 Semibenzilic rearrangement.

semibenzilic mechanism have been reported, even for compounds with hydrogen available for enolization.[7] The cyclopropanone mechanism usually works, in preference to the semibenzilic mechanism. In several examples, a symmetrical intermediate is involved. The occurrence of a symmetrical intermediate has also been demonstrated by ^{14}C labeling in the case of α-chlorocyclohexanone,[8] as shown in Scheme 3. The reaction in Scheme 3 may occur either *via* the semibenzilic acid mechanism (route A, Scheme 4) or *via* the cyclopropanone mechanism (route B, Scheme 5).

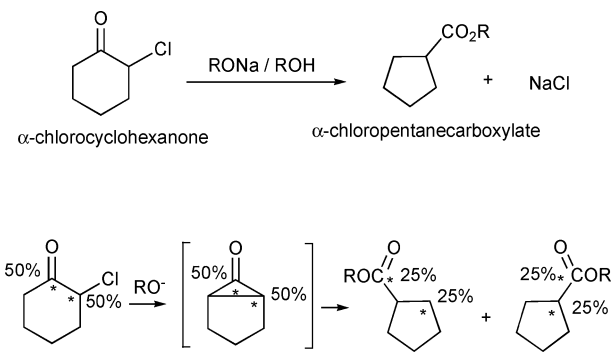

Scheme 3 A representative Favorskii rearrangement and the result of the isotope labeled compound. Asterisks are attached to ^{14}C labeled atoms.[8]

Five theoretical studies of the Favorskii rearrangement have been reported.[9] Among them, reaction paths of the two competitive mechanisms (A and B) were investigated first by the use of α-chlorobutanone and a hydroxide ion.[9c] ts3B (after the bicyclobutanone intermediate, on the left in Scheme 6) has a high energy, and route A was reported to be more likely than

Department of Chemistry, Nara University of Education, Takabatake-cho, Nara, 630-8528, Japan. E-mail: yamabes@nara-edu.ac.jp

† Electronic supplementary information (ESI) available: Reactant, intermediates and product geometries, reaction-coordinate vectors corresponding to respective sole imaginary frequencies for TSs and geometries of $MeO^-(MeOH)_{11}$ and $Na^+(MeOH)_{11}MeO^-$ (Fig. S1–S8). Cartesian coordinates of the optimized geometries of Fig. 1, 2 and 4. See DOI: 10.1039/b806577b

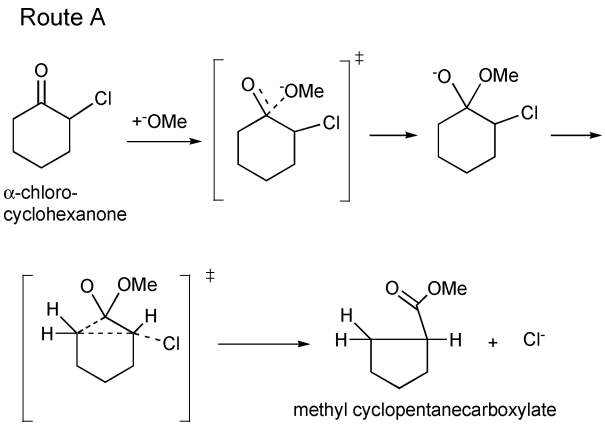

Scheme 4 The semibenzilic acid mechanism for Scheme 3 proposed by Tchoubar and Sackur.[7]

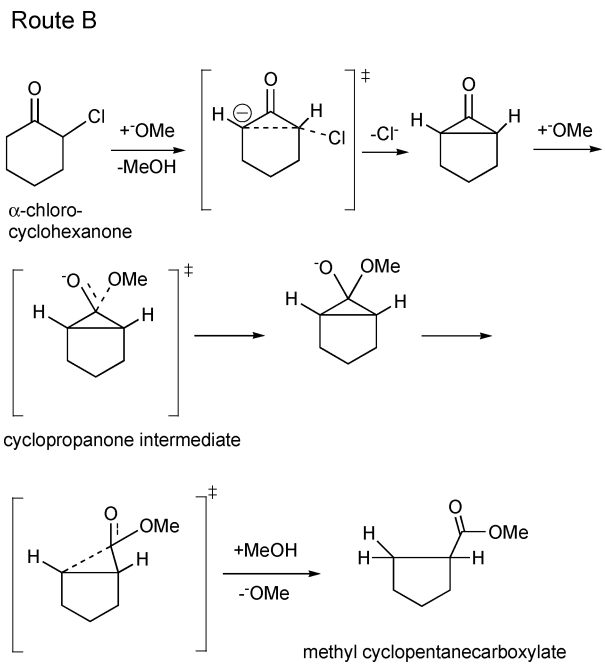

Scheme 5 The cyclopropanone mechanism for Scheme 3 proposed by Loftfield.[8]

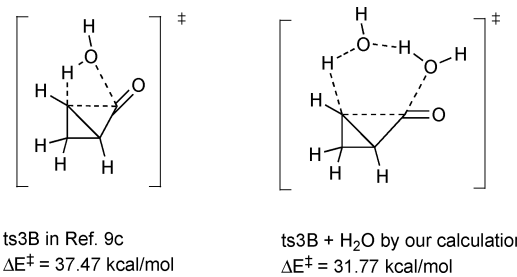

Scheme 6 Transition state (TS) structures of the H_2O (or $2H_2O$) addition to bicyclopropanone, which was obtained in this work. $\Delta E^{\ddagger}$ is the energy difference between ts3B (or ts3B + H_2O) and the preceding intermediate, I2B (or I2B + H_2O). The calculated TS geometries are shown in Fig. S1 (ESI†). The dissociated Cl^- was omitted in TS calculations.

route B. Paths A and B for a model (α-chlorocyclohexanone and OH^-) were also reported,[9d] where ts3B has a similar four-centered geometry. In general, the four-centered addition path is energetically unfavorable. In our previous studies,[10] the four-centered path was computed to be much less favorable than the water dimer or trimer participating path. The hydrogen-bond circuit promoting proton relays in the dimer or trimer may lower the activation energy considerably. The generality is checked by the use of ts3B. The activation energy, $\Delta E^{\ddagger} = 37.47$ kcal mol^{-1}, of ts3B is larger than $\Delta E^{\ddagger} = +31.77$ kcal mol^{-1} of ts3B + H_2O (Scheme 6). In ts3B + H_2O, the water dimer is involved in the addition, and the ring strain in the TS structure is relaxed through proton relays and the nucleophilic addition ($HO^- \rightarrow C{=}O$). Thus, the cyclopropanation mechanism needs to be investigated in explicit consideration of proton relays along hydrogen bonds.

In this work, the representative Favorskii rearrangement, α-chlorocyclohexanone and MeO^- in methanol (MeOH) solvent, was studied computationally. Since the hydrogen bonds have a crucial role on the rearrangement, eight MeOH molecules were included explicitly in the reacting system. Scheme 7 illustrates how they are coordinated with lone-pairs of the substrate (α-chlorocyclohexanone) and the nucleophilic reagent (MeO^-). It will be shown that the cyclopropanone mechanism has a surprising new elementary process.

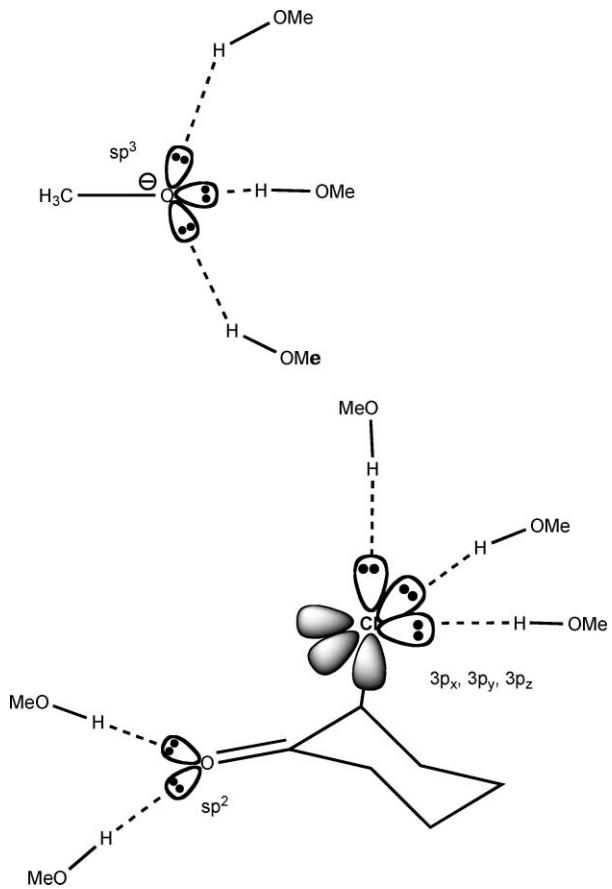

Scheme 7 A present model simulating the reaction in Scheme 3, which is composed of α-chlorocyclohexanone, a methoxide ion and eight methanol molecules. Each MeOH molecule is linked with a lone-pair orbital in the hydrogen bond.

2 Methods of calculation

The geometries of the reactants were determined by density functional theory calculations. The B3LYP method[11] was used. B3LYP is a suitable method, because it includes the electron correlation effect to some extent.[12] The basis set employed is 6-31G*. Since the size of the reacting system in Scheme 7 is very large, methyl groups were approximated by the semiempirical method, PM3, and the ONIOM (RB3LYP/6-31G*:PM3)[13] calculations were carried out. Thus, nine methyl groups were treated by PM3 and other parts were treated by RB3LYP/6-31G* for the reacting systems. Furthermore, RB3LYP/6-31(++)G(d,p) geometry optimization of TS2A, TS2B and TS4B were made for a model of α-chlorocyclohexanone and $MeO^-(MeOH)_6$.

Transition states (TSs) were characterized by vibrational analysis, which checked whether the obtained geometries have single imaginary frequencies ($\nu^{\ddagger}$s). The geometries and the Hessian force constants at the TSs were used for the subsequent geometry optimizations of precursors and products.

Single-point RB3LYP/6-311+G(d,p) SCRF=dipole[14] (solvent MeOH, dielectric constant = 32.63) energy calculations were made, and internal energies (T = 0 K) were estimated by the sum of the ONIOM zero point vibrational energy correction and the single-point energy. The RB3LYP/6-311+G(d,p) SCRF=dipole//RBLYP/6-31G*-ONIOM method is reliable in view of computational results of related studies. The splicing way is recommended to gain energies close to experimental ones.[12] The B3LYP method has been applied to hydrogen-bonded systems. The HOH–OH_2 hydrogen-bond energy was calculated to be 3.02 kcal mol^{-1} by RB3LYP/cc-pVDZ,[15] which is in good agreement with the experimental energy, 3.59 kcal mol^{-1}.[16] The FH–FH energy was calculated to be 2.68 kcal mol^{-1} by RB3LYP/6-311+G(2df,p),[17] while the experimental value was 3.02 ± 0.02 kcal mol^{-1}.[18] The HCN–HF energy was 6.35 kcal mol^{-1},[19] and the experimental value was 6.9 kcal mol^{-1}.[20] Thus, the computational method is applicable to reacting systems including hydrogen bonds. RB3LYP/6-311++G(d,p) SCRF=dipole and MP2/6-311++G(d,p) single-point calculations were also carried out for four key TSs: TS2A, TS2B, TS3B and TS4B. All the calculations were carried out using the GAUSSIAN 03[21] program package. The computations were performed using the Research Center for Computational Science, Okazaki, Japan.

3 Results and discussion

Fig. 1 shows the route of the semibenzilic acid mechanism (A). The first step is a nucleophilic MeO^- addition to the carbonyl carbon of the substrate (TS1A). Noteworthy is that TS1A involves a one-center addition (O18→C6) and a concomitant proton relay (O18–H19 ··· O20 → O18 ··· H19–H20). Without the relay, transition state structures could not be found. After TS1A, a Meisenheimer complex (IntA) is afforded, which is slightly more stable than the precursor ($\Delta E = -1.07$ kcal mol^{-1}). From IntA, the second TS, TS2A, could be successfully obtained. In TS2A, cleavage of C(1)–Cl(9) and C(6)–C(5) covalent bonds and formation of C(1)–C(5) occur simultaneously. After TS2A, the product geometry was obtained. In Fig. 1, the MeOH solvent molecule has an active role (*i.e.*, proton relay) on TS1A.

Fig. 2 shows route B (cyclopropanone mechanism). The first step is α′ proton removal (TS1B) with a small activation energy, $\Delta E^{\ddagger}$ = +1.85 kcal mol^{-1}, in spite of the C–H bond cleavage. A carbanion intermediate, Int1B, is formed. The intermediate is susceptible to intramolecular nucleophilic displacement, TS2B, which leads to the cyclopropanone intermediate, Int2B. The intermediate Int2B undergoes MeOH addition accompanied by proton relays, TS3B. While the reactivities of $n = 2$ and $n = 3$ are competitive in Scheme 8, the TS geometry optimization for TS3B in Fig. 2 gave uniquely the $(MeOH)_3$ participation. After TS3B, the cyclopentane product (product′) is yielded. The primes attached to the precursor (precursor′) and the product (product′) represent a hydrogen-bonded complex of $(MeOH)_8$ slightly different from that in Fig. 1.

Fig. 3 exhibits energy changes along routes A (Fig. 1) and B (Fig. 2). The rate-determining step of route A is TS2A, and that of route B is TS3B. Their activation energies are 33.79 kcal mol^{-1} (TS2A) and 31.29 kcal mol^{-1} (TS3B), respectively, which are too large for the Favorskii rearrangement to occur readily. Alternative paths of the smaller activation energies need to be sought.

One possibility of an alternative path is nucleophilic attack of the cyclopropanone intermediate by the evolved chloride ion, which has not been considered so far. The second MeO^- attack (Scheme 9) described in the textbook[22] would be improbable for the following three reasons: the first is that the Cl^- ion released at TS2B (Fig. 2) would remain at the reacting region surrounded by MeOH clusters *via* hydrogen bonds. The large-sized anion would block approach of the second MeO^- ion. The second is that the Favorskii rearrangement is known to follow a second-order rate equation (*i.e.*, the first order with respect to the concentration of MeO^-).[23] Since TS3B (or an alternative path) is obviously rate-determining, the second MeO^- participation shown in Scheme 9 would give the third-order rate equation. The third is a rule in S_N reactions, and states that the nucleophile with the most freedom has the larger nucleophilicity.[22] In polar protic solvents, *e.g.* water and methanol, the nucleophilicity order is $I^- > Br^- > Cl^- > F^-$, whereas in the gas phase, the order is $I^- < Br^- < Cl^- < F^-$. In this respect, the order between MeO^- and Cl^- in the present reaction is also solvation controlled, and the Cl^- ion would be a good nucleophile.

Scheme 9 might have been suggested in the sense that the cyclopropanone ring needs to be cleaved by a strong and anionic nucleophile. In fact, the concerted path, TS3B, by the neutral $(MeOH)_3$ cluster has a large activation energy ($\Delta E^{\ddagger}$ = 31.29 kcal mol^{-1} in Fig. 3). Then, the Cl^- attack model shown in Scheme 10 is a candidate for an alternative path. The nucleophile Cl^- attack and the proton attack would occur either at the same time (TS4B in Scheme 10) or in a stepwise mode similar to that of Scheme 9. An acetyl chloride intermediate, Int3B, would be formed. Int3B contains the MeO^- ion, and an instantaneous nucleophilic displacement (TS5B) would occur. The product (product″) is afforded. Reaction paths that followed Scheme 10 were traced, and they are exhibited in Fig. 4. TS4B was computed to have the simultaneous occurrence of Cl(16)–C(6) and C(5)–H(17) bond formation and C(5)–C(6) bond cleavage. The operation of Cl^- expected in Scheme 10 was obtained successfully in Fig. 4. Fig. 5 shows the energy change, including our new mechanism

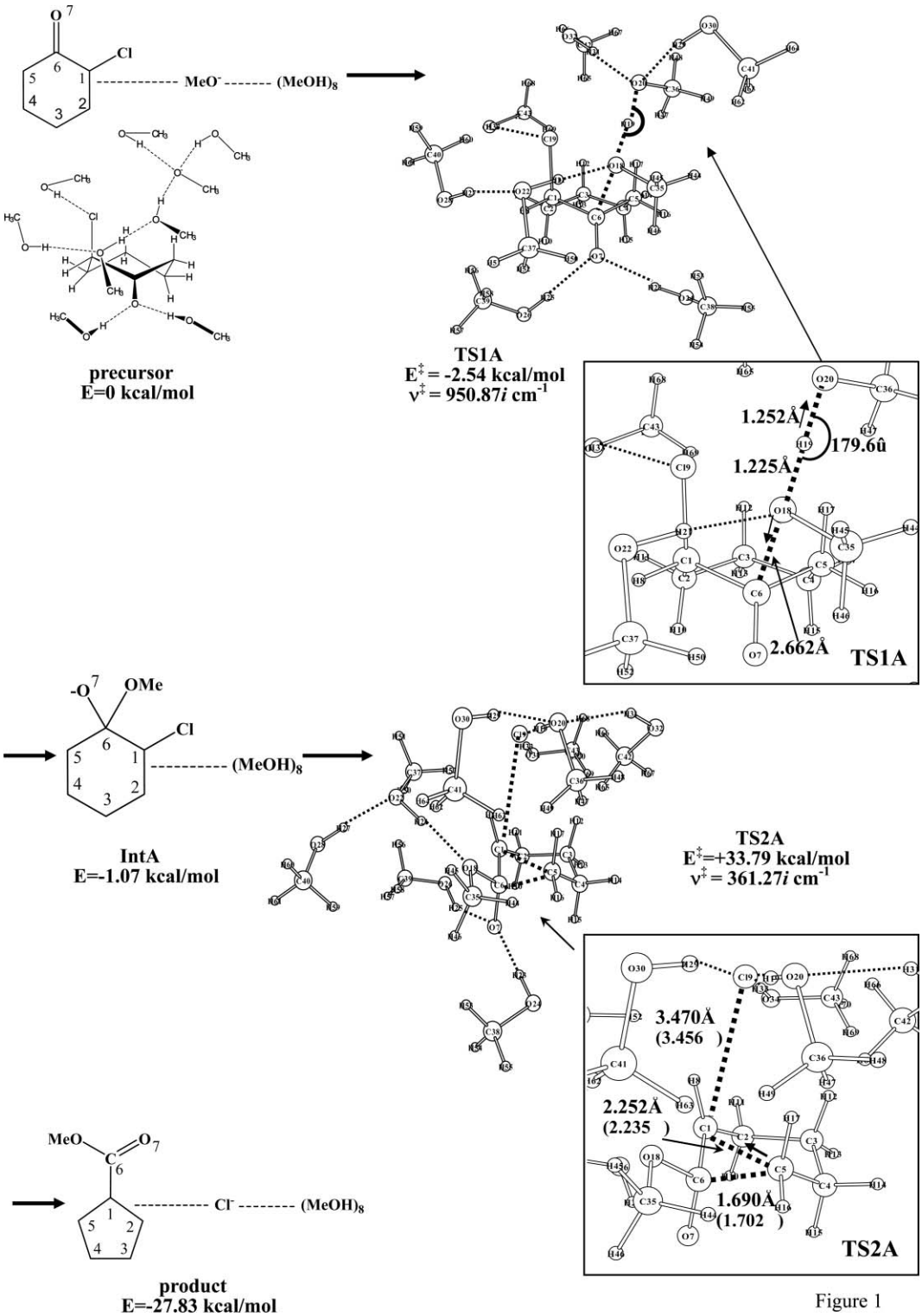

Figure 1

Fig. 1 The reaction route of the semibenzilic acid mechanism, which is composed of α-chlorocyclohexanone, a methoxide ion and eight MeOH molecules. For TS1A and TS2A, larger scale figures are shown in the boxes. In the precursor, IntA and product, broken lines denote that weak attractive interactions are involved. ΔE is the energy difference relative to that of the precursor ($\Delta E > 0$, less stable). $\nu^{\ddagger}$ is the sole imaginary frequency, which verifies that the obtained geometry is correctly located at the saddle point. Geometries of precursor, IntA and product are exhibited in Fig. S2 in the ESI.† The bond distances in TS2A in parentheses are those calculated by RB3LYP/6-31(++)G(d,p) by the use of a model TS2A′ composed of α-chlorocyclohexanone and $MeO^{-}(MeOH)_6$, where "(++)" means that diffuse orbitals were added to oxygen, chlorine and hydroxyl hydrogens. Geometries of TS2A′ are exhibited in Fig. S8 in the ESI.

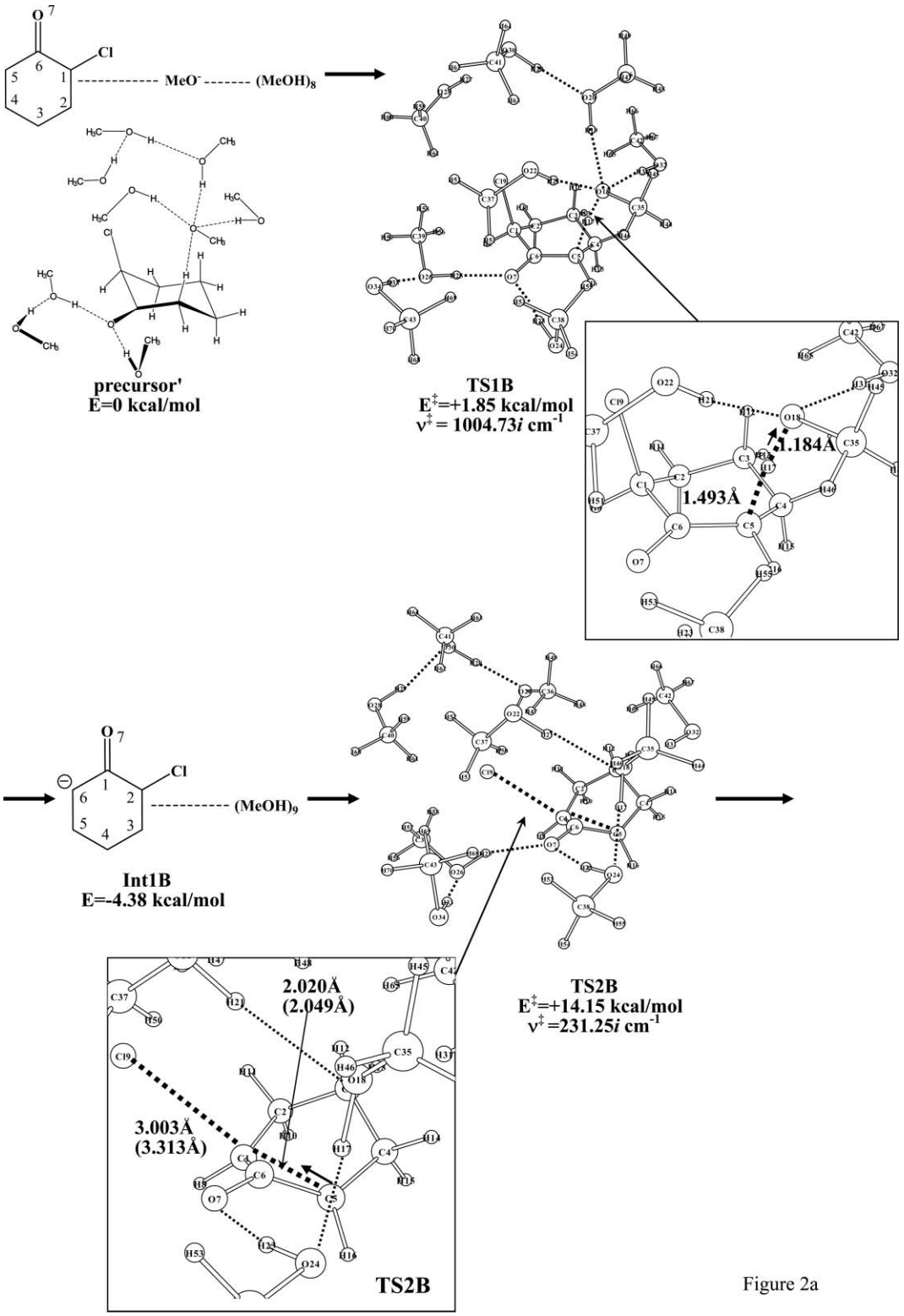

Figure 2a

Fig. 2a The route of the cyclopropanone mechanism. Int2B is the cyclopropanone intermediate. Precursor′ and product′ in Fig. 2 are isomers of the precursor and product in Fig. 1, respectively; the difference is in the hydrogen-bond pattern. Geometries of precursor′, Int1B, Int2B and product′ are exhibited in Fig. S3 in the ESI.† The bond distances in TS2B in parentheses are those calculated by RB3LYP/6-31(++)G(d,p) by the use of a model TS2B′ composed of α-chlorocyclohexanone and $MeO^{-}(MeOH)_6$. Geometries of TS2B′ are exhibited in Fig. S8 in the ESI.

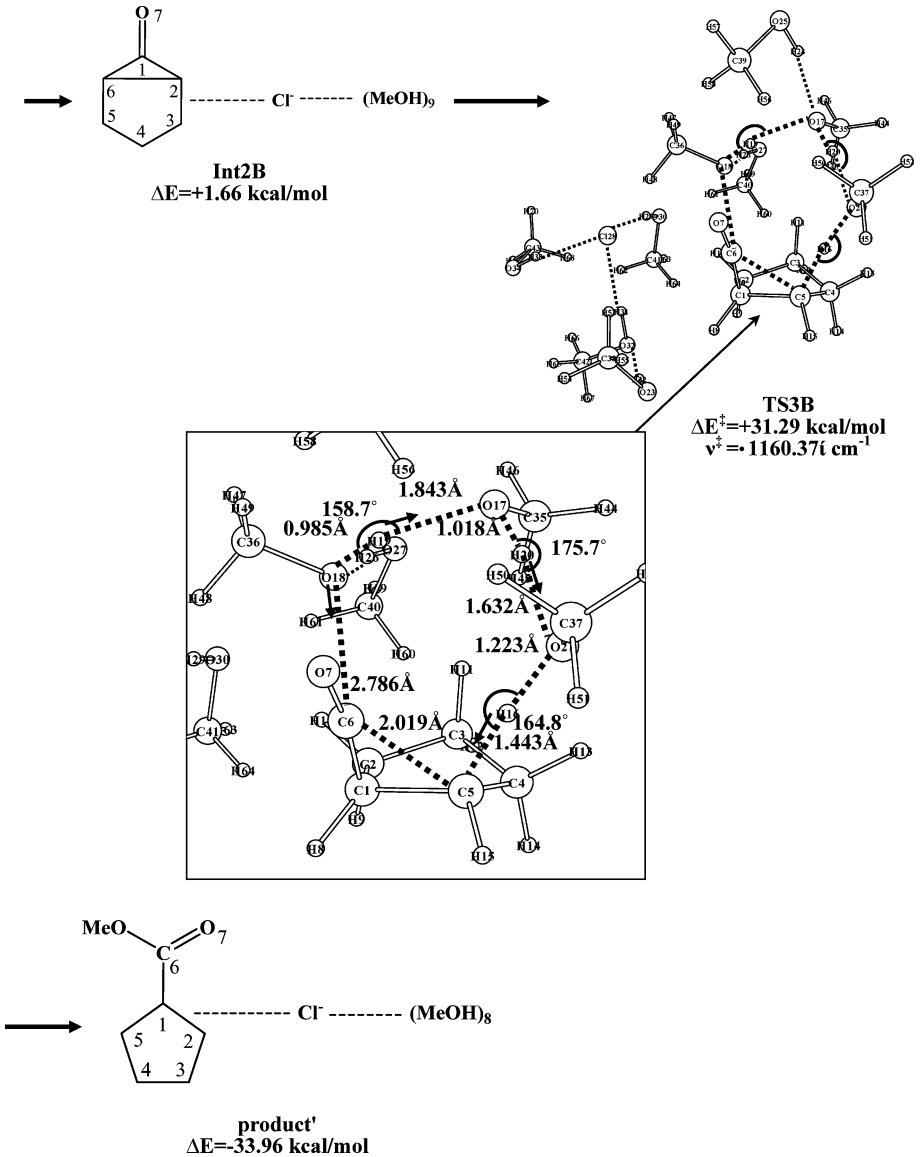

Fig. 2b

of Scheme 10, and Fig. 4 at the latter stage of the Favorskii rearrangement. The energy change of the former stage is taken from Fig. 3. TS4B (Cl^- attack on cyclopropanone) is found to be the rate-determining step by RB3LYP SCRF=dipole single-point energies.[24] TS4B has a much smaller activation energy (= +17.75 kcal mol^{-1}) than that in Fig. 3 (= +31.29 kcal mol^{-1} of TS3B). Our Cl^- recovery paths starting from the cyclopropanone intermediate are found to be likely.

The salt effect is considered, because the standard reactant is Na^+OMe^- in MeOH as shown in Scheme 3. Scheme 11 shows the geometry of $NaOMe(MeOH)_{11}$. The sodium ion is tetrahedrally coordinated, and the three lone-pair orbitals of the methoxide ion are hydrogen bonded with O–H distances of 1.479, 1.512 and 1.525 Å. These in $MeO^-(MeOH)_{11}$ are 1.488, 1.519 and 1.523 Å, as shown in Fig. S6 of the ESI.† The similar distances demonstrate that the counter ion Na^+ is strongly solvated and the ion does not strengthen hydrogen bonds around MeO^-. Thus, the present Na^+-free model seems to give a similar result to the Na^+ containing models.

4 Concluding remarks

This work has dealt with the representative Favorskii rearrangement, α-chlorocyclohexanone and MeO^-/MeOH by ONIOM-DFT calculations. Eight MeOH molecules linked with lone-pair orbitals of heteroatoms contained in the substrate were included explicitly in the geometry optimizations. The semibenzilic acid mechanism (A) is energetically unlikely. The cyclopropanone mechanism (B) is more favorable than A, but B has a rate-determining step, TS3B, of a large activation energy. TS3B consists of a concerted MeO^-, and proton addition to a cyclopropanone intermediate by an MeOH trimer. An alternative route from the intermediate has been proposed in Scheme 10. In the route, the chloride ion evolved at TS2B works as a nucleophile toward

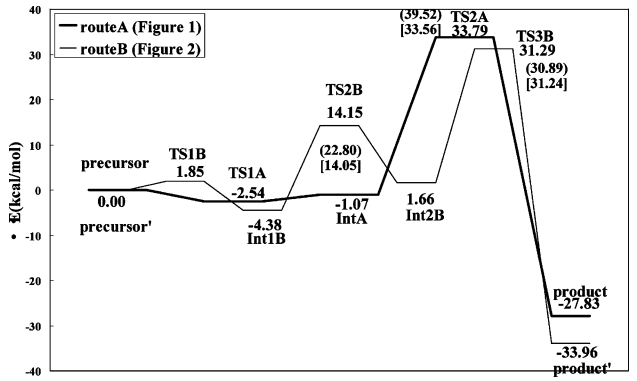

Fig. 3 Energy changes (energies relative to those of precursor and precursor′) along the routes in Fig. 1 and 2, which were obtained by differences of the sum of RB3LYP/6-311+G(d,p) SCRF=dipole electronic energy and ONIOM(RB3LYP/6-31G*:PM3) ZPE. The sum total energies of precursor and precursors′ are −1810.40644480 a.u. and −1810.40010097 a.u., respectively. Its difference comes from hydrogen-bond patterns as shown in Fig. S2-1 and S3-1 (ESI†). Since the difference is apart from the reactivity, those total energies are taken to be zero commonly as the starting point. The activation energy −2.54 kcal mol^{-1} of TS1A was calculated. The negative value arises from the way of evaluating relative energies, *i.e.*, differences of RB3LYP/6-311+G(d,p) single-point electronic and OINOM zero-point vibrational energies. In the ONIOM electronic energy, the activation value of TS1A is +2.17 kcal mol^{-1}. The values of TSs (TS2A, TS2B and TS3B) in parentheses and in square brackets are from single-point energy calculations by RB3LYP/6-311++G(d,p) SCRF=dipole and MP2/6-311++G(d,p) methods, respectively.

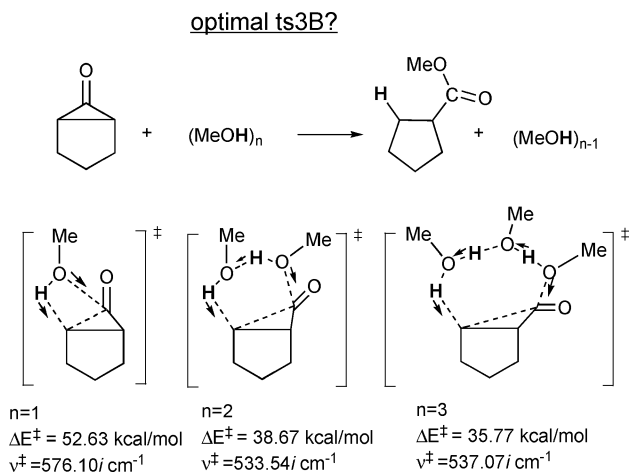

Scheme 8 Concerted proton relays in MeOH addition to the cyclopropanone intermediate. The $n = 4$ addition path could not be obtained, probably owing to the narrow C–C bond region. The detailed geometries are shown in Fig. S5 in the ESI.†

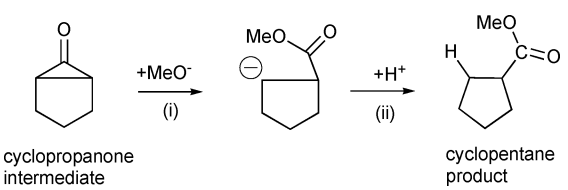

Scheme 9 A stepwise path, (i) MeO$^-$ addition and (ii) the consequent H$^+$ addition, illustrated in a textbook of organic reactions.[22]

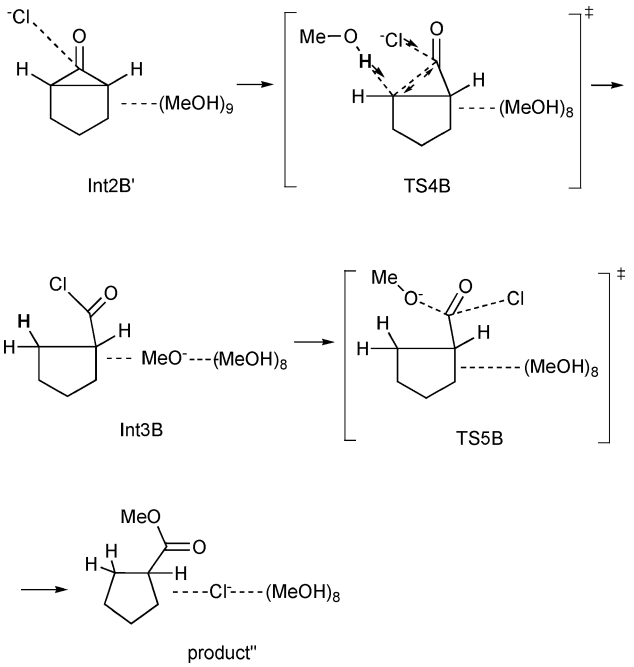

Scheme 10 An alternative path from the cyclopropanone intermediate, Int2B′, to the cyclopentane product, product″. TS4B and TS5B are of the nucleophilic displacement.

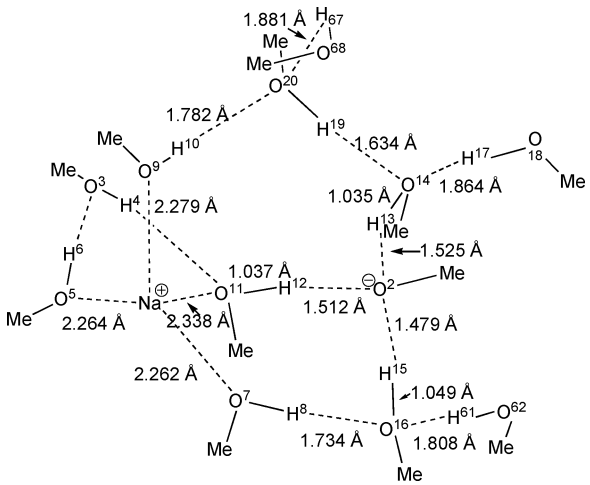

Scheme 11 An ion pair model of $Na^+(MeOH)_{11}MeO^-$. The optimized geometry is given in Fig. S7 of the ESI.†

the intermediate. Our new mechanism involves an acyl chloride intermediate being susceptible to subsequent MeO$^-$ attack, leading to the product. In Fig. 5, the Favorskii rearrangement has three intermediates, and the rate-determining step is TS4B. The rearrangement route is summarized in Scheme 12. In the modified cyclopropanone mechanism, the chloride ion is a leaving group, and at the same time a nucleophile. Although the semibenzilic mechanism is unfavorable at TS2A (Fig. 3), IntA with a small activation energy (= +2.77 kcal mol^{-1}) is yielded readily. IntA is a Meisenheimer complex and may coexist in equilibrium with the precursor. The coexistence disappears eventually by the non-equilibrium cyclopropanone route according to Le Chatelier's law. The rearrangement is thought to be described

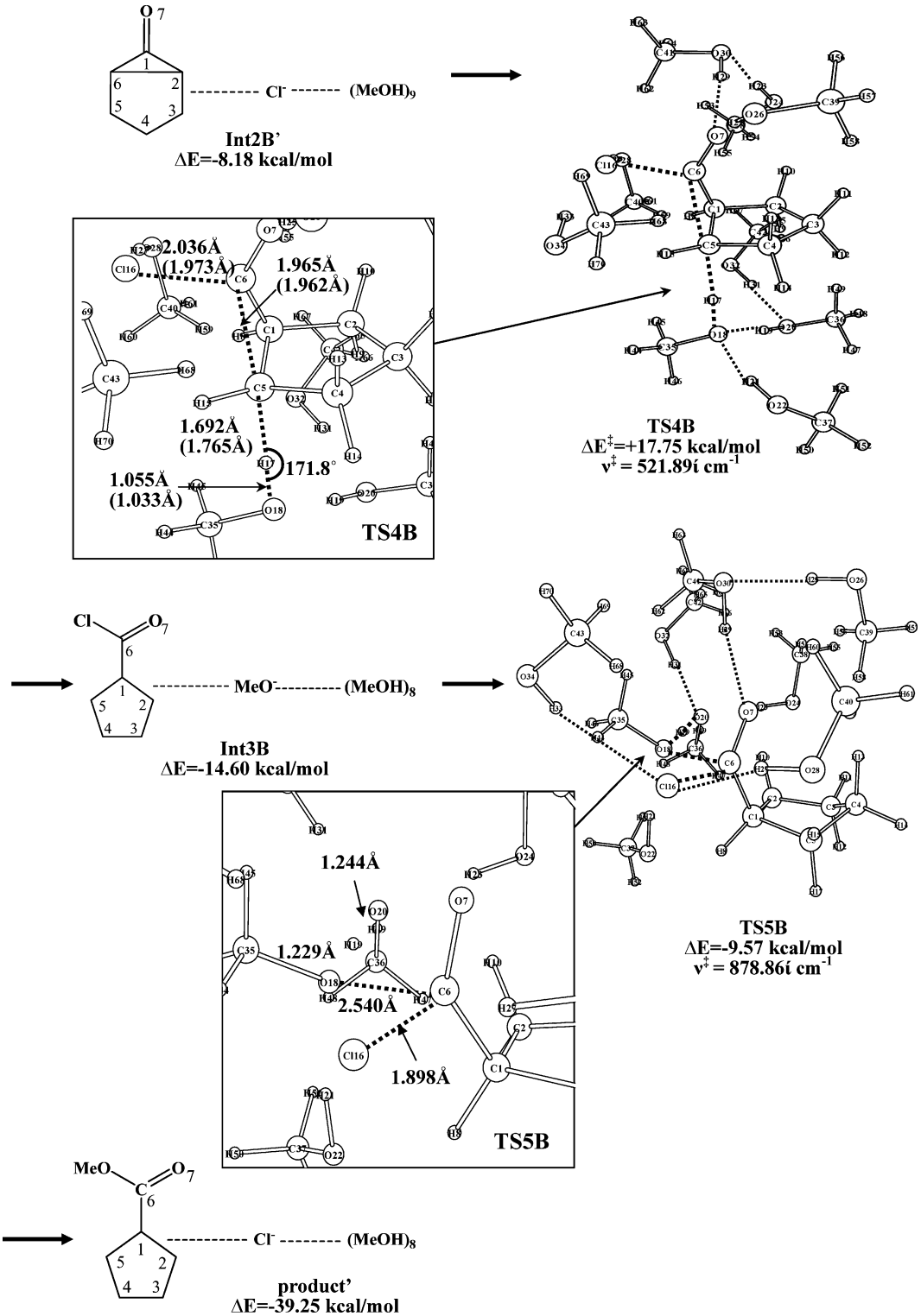

Fig. 4 An alternative route of Scheme 10. Int2B′ and product″ are isomers of Int2B and product′ in Fig. 2, respectively; differences are in the hydrogen-bond pattern. Geometries of Int2B′, Int3B and product″ are exhibited in Fig. S4 in the ESI.† The bond distances in TS4B in parentheses are those calculated by RB3LYP/6-31(++)G(d,p) by the use of a model TS4B′ composed of α-chlorocyclohexanone and $MeO^-(MeOH)_6$. Geometries of TS4B′ are exhibited in Fig. S8 in the ESI.

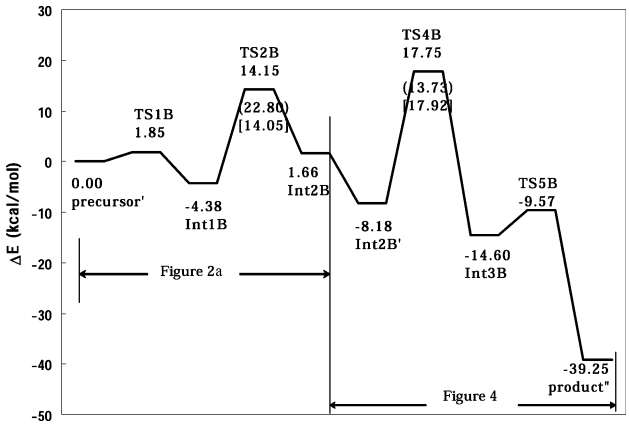

Fig. 5 Energy changes along the route of Fig. 1, 2a and 4. The values of TS2B and TS4B in parentheses and in square brackets are from single–point energy calculations by RB3LYP/6-311++G(d,p) SCRF=dipole and MP2/6-311++G(d,p) methods, respectively.

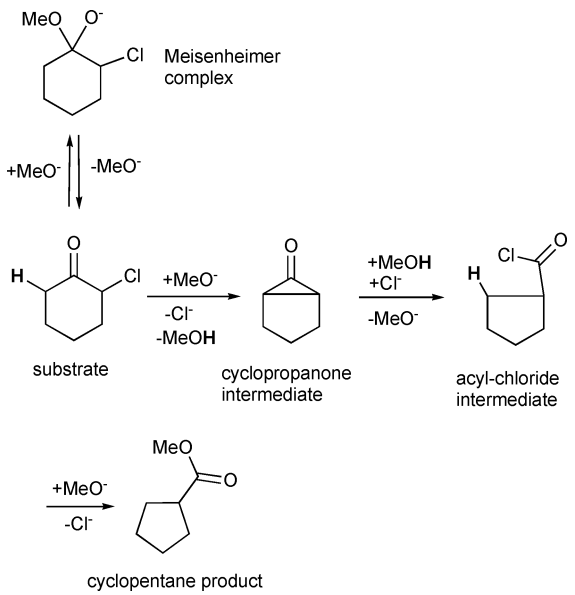

Scheme 12 A new mechanism of the Favorskii rearrangement, which involves an acyl chloride intermediate.

correctly in terms of proton attack or removal *via* hydrogen bonds by the present $(MeOH)_8$-containing model.

In the present work, an innovative pattern of ionic reactions is presented; in the early stage, the leaving group becomes a negative ion, and it becomes a nucleophilic reagent at the later stage.

References

1 A. E. Favorskii, *J. Russ. Phys. Chem. Soc.*, 1894, **26**, 559.
2 A. S. Kende, *Org. React.*, 1960, **11**, 261.
3 F. A. Carey and R. J. Sundberg, *Advanced Organic Chemistry*, Plenum Press, New York, 1990, 3rd edn, part B, ch. 10.
4 (*a*) E. Lee and C. H. Yoon, *J. Chem. Soc., Chem. Commun.*, 1994, 47; (*b*) J. M. Llera and B. Fraser-Reid, *J. Org. Chem.*, 1989, **54**, 5544.
5 (*a*) H. Takeshita, H. Kawakami, Y. Ikeda and A. Mori, *J. Org. Chem.*, 1994, **59**, 6490; (*b*) P. E. Eaton and T. W. Cole, *J. Am. Chem. Soc.*, 1964, **86**, 962.
6 (*a*) F. G. Bordwell, T. G. Scamehorn and W. R. Springer, *J. Am. Chem. Soc.*, 1969, **91**, 2087; (*b*) F. G. Bordwell and J. G. Strong, *J. Org. Chem.*, 1973, **38**, 579.
7 (*a*) B. Tchoubar and O. Sackur, *Compt. Rend.*, 1939, **208**, 1020; (*b*) E. W. Warnhoff, C. M. Wong and W. T. Tai, *J. Am. Chem. Soc.*, 1968, **90**, 514.
8 (*a*) R. B. Loftfield, *J. Am. Chem. Soc.*, 1950, **72**, 632; (*b*) R. B. Loftfield, *J. Am. Chem. Soc.*, 1951, **73**, 4707.
9 (*a*) L. D. Schaad, B. A. Hess and R. Zahradnik, *J. Org. Chem.*, 1981, **46**, 1909; (*b*) L. E. Boyer, J. Brazzillo, M. A. Forman and B. Zanoni, *J. Org. Chem.*, 1996, **61**, 7611; (*c*) V. Moliner, R. Castillo, V. S. Safont, M. Oliva, S. Bohn, I. Tunon and J. Andres, *J. Am. Chem. Soc.*, 1997, **119**, 1941; (*d*) R. Castillo, J. Andres and V. Moliner, *J. Phys. Chem. B*, 2001, **105**, 2453; (*e*) G. D. Hamblin, R. P. Jimenez and T. S. Sorensen, *J. Org. Chem.*, 2007, **72**, 8033.
10 (*a*) S. Yamabe, N. Tsuchida and K. Miyajima, *J. Phys. Chem. A*, 2004, **108**, 2750; (*b*) N. Tsuchida and S. Yamabe, *J. Phys. Chem. A*, 2005, **109**, 1974; (*c*) S. Yamabe, N. Tsuchida and Y. Hayashida, *J. Phys. Chem. A*, 2005, **109**, 7216.
11 (*a*) A. D. Becke, *J. Chem. Phys.*, 1993, **98**, 5648; (*b*) C. Lee, W. Yang and R. G. Parr, *Phys. Rev. B*, 1998, **37**, 785.
12 J. B. Foresman and Æ. Frisch, *Exploring Chemistry with Electronic Structure Methods*, Gaussian Inc., Pittsburgh, 1996, 2nd edn, ch. 7.
13 F. Maseras and K. Morokuma, *J. Comput. Chem.*, 1995, **16**, 1170.
14 L. Onsager, *J. Am. Chem. Soc.*, 1936, **58**, 1486.
15 O. Isayev, L. Gorb and J. Leszczynski, *J. Comput. Chem.*, 2007, **28**, 1598.
16 L. A. Curtiss, D. J. Frurip and M. Blander, *J. Chem. Phys.*, 1979, **71**, 2703.
17 K. N. Rankin and R. J. Boyd, *J. Comput. Chem.*, 2001, **22**, 1590.
18 (*a*) B. J. Howard, T. R. Dyke and W. Klemperer, *J. Chem. Phys.*, 1984, **81**, 5417; (*b*) H. S. Gutowsky, C. Chuang, J. D. Keen, T. D. Klots and T. Emilsson, *J. Chem. Phys.*, 1985, **83**, 2070.
19 S. Tsuzuki and H. P. Lüthi, *J. Chem. Phys.*, 2001, **114**, 3949.
20 B. A. Wofford, M. E. Eliades, S. G. Lieb and J. W. Bevan, *J. Chem. Phys.*, 1987, **87**, 5674.
21 *Gaussian 03*, Revision C.02, M. J. Frisch, G. W. Trucks, H. B. Schlegel, G. E. Scuseria, M. A. Robb, J. R. Cheeseman, J. A. Montgomery, Jr., T. Vreven, K. N. Kudin, J. C. Burant, J. M. Millam, S. S. Iyengar, J. Tomasi, V. Barone, B. Mennucci, M. Cossi, G. Scalmani, N. Rega, G. A. Petersson, H. Nakatsuji, M. Hada, M. Ehara, K. Toyota, R. Fukuda, J. Hasegawa, M. Ishida, T. Nakajima, Y. Honda, O. Kitao, H. Nakai, M. Klene, X. Li, J. E. Knox, H. P. Hratchian, J. B. Cross, V. Bakken, C. Adamo, J. Jaramillo, R. Gomperts, R. E. Stratmann, O. Yazyev, A. J. Austin, R. Cammi, C. Pomelli, J. W. Ochterski, P. Y. Ayala, K. Morokuma, G. A. Voth, P. Salvador, J. J. Dannenberg, V. G. Zakrzewski, S. Dapprich, A. D. Daniels, M. C. Strain, O. Farkas, D. K. Malick, A. D. Rabuck, K. Raghavachari, J. B. Foresman, J. V. Ortiz, Q. Cui, A. G. Baboul, S. Clifford, J. Cioslowski, B. B. Stefanov, G. Liu, A. Liashenko, P. Piskorz, I. Komaromi, R. L. Martin, D. J. Fox, T. Keith, M. A. Al-Laham, C. Y. Peng, A. Nanayakkara, M. Challacombe, P. M. W. Gill, B. Johnson, W. Chen, M. W. Wong, C. Gonzalez and J. A. Pople, Gaussian, Inc., Wallingford CT, 2004.
22 See for example: M. B. Smith, J. March, *March's Advanced Chemistry, Reactions, Mechanisms, and Structure*, Wiley, New Jersey, 2007, 6th edn.
23 P. Sykes, *The Search for Organic Reaction Pathways*, Longman Group Limited, London, 1972, ch. 6b.
24 MP2/6-311++G(d,p) single-point energies, however, indicate that TS2B is rate-determining with (22.80 kcal mol^{-1}). They do not include the SCRF solvent effect, and probably the effect would lower the energy. SCRF=dipole containing MP2/6-311++G(d,p) calculations could not be carried out. Since TS2B involves scission of only the C–Cl bond, it cannot be rate-determining. Besides the solvent effect, the MP2/6-311++G(d,p) TS might be somewhat different from the B3LYP ones.